IEEE Access
Multidisciplinary : Rapid Review : Open Access Journal

Received 8 November 2023, accepted 18 December 2023, date of publication 4 January 2024, date of current version 29 January 2024.

Digital Object Identifier 10.1109/ACCESS.2024.3349951

RESEARCH ARTICLE

Endmember Analysis of Overlapping Handwritten Text in Hyperspectral Document Images

HASAN IRTAZA MIRZA[1], SAAD BIN AHMED[2], ROBERTO SOLIS-OBA[3], AND MUHAMMAD IMRAN MALIK[1]
[1]School of Electrical Engineering and Computer Science, National University of Sciences and Technology (NUST), Islamabad 44000, Pakistan
[2]Department of Computer Science, Faculty of Science and Environmental Studies, Lakehead University, Thunder Bay, ON P7B 5E1, Canada
[3]Department of Computer Science, Middlesex College, University of Western Ontario, London, ON N6A 3K7, Canada

Corresponding author: Saad Bin Ahmed (sbinahm@lakeheadu.ca)

The work of Saad Bin Ahmed was supported in part by the Centre for Advanced Studies in Engineering and Sciences, Lakehead University. The work of Roberto Solis-Oba was supported in part by the Natural Sciences and Engineering Research Council of Canada under Grant RGPIN 2020-06423.

ABSTRACT Hyperspectral Imaging (HSI) uses large portions of the electromagnetic spectrum to obtain information from images that would be very difficult to get otherwise. An important task in forensic analysis of documents is to extract signatures for authentication. Signatures in documents often overlap with other parts of a document such as typed text or stamps and hence it is difficult to retrieve them. In this work we present a novel algorithm for recovering signatures from hyperspectral images of documents where signatures overlap typed text, seals, stamps, or other images. We used pure pixel index approaches to analyze the hyper-pixels corresponding to regions where overlaps occur and spectral classification methods to analyze the extracted channels' information and to separate the overlapping signatures. We used the structural similarity index to validate the extracted signatures. Our experimental results highlight the capability of the proposed algorithm to recover signatures with great precision in HSI document images.

INDEX TERMS Hyperspectral imaging, endmembers, spectrum, abundance estimation, spectral analysis.

I. INTRODUCTION

Hyperspectral imaging (HSI) uses the entire electromagnetic spectrum for performing tasks such as identifying objects in images [1], [2]. HSI has already gained popularity in various fields like astronomy, medicine, chemical analysis and industrial quality control [3]. HSI is inspired from nature where many animals make effective use of wavelengths outside the visible region to detect and classify objects. For example, honey bees and butterflies can see in the ultraviolet spectrum and gold fish can see light both in infrared and ultraviolet spectra. Spectroscopy studies the relationship between light and matter. It investigates how a target material can be recognized from its spectral characteristics, called its spectral signature. HSI images are captured by a special camera called image spectrometer which collects spectral information. Using hyperspectral cameras we can capture hundreds of thousands of wavelengths or spectral bands. Each pixel in an HSI image contains information from the full spectral range of the camera. This allows, for example, the possibility of recovering information of individual overlapping objects in an HSI image.

This paper explores the idea of analyzing hyperspectral images of documents containing overlapping images and, typed and handwritten text for segmenting the pixels comprising the handwritten text. Extracting handwritten text and signatures from machine printed documents is important for forensic document analysis [1] and efficient document retrieval [2].

Separating overlapping handwritten text, images, and typed text in an RGB image is difficult as text and images might use the same colors, which could result in the loss of important information when separating them. Intuitively, it should be possible to segment regions with overlapping text

The associate editor coordinating the review of this manuscript and approving it for publication was Gangyi Jiang.

and images by using information from the whole range of the electromagnetic spectrum and taking advantage of their different spectral properties.

The contributions of this work proposed work are as follows,

- This paper presents a methodology for overlapping text segmentation in HSI images using pure pixel index methods. Our experimental results show that our algorithm can extract with high accuracy signatures from documents, even when the signatures overlap typed text and images (like stamps or seals).
- To measure the fidelity of the extracted signatures we propose the use of the Structural Similarity Index Measure (SSIM) [3], which gives an accurate measurement of the similarity of the extracted signatures with the actual ones. The use of SSIM has advantages over error-sensitivity approaches that traditionally have been used to measure the quality of extracted signatures, including elimination of low correlation between images fidelity and image quality.

This paper is organized as follows. Related work is summarized in Section II. Sections III and IV explains spectral unmixing and spectral similarity methods. Sections V and VI describe our model for HSI document processing and the evaluation metrics that we used. Our experimental analysis is presented in Section VII. Conclusions are presented in Section VIII.

II. RELATED WORK

In forensic document analysis, signature detection and extraction are important steps prior to signature verification. An approach for detecting and extracting signatures from machine-printed documents is presented in [1] that identifies signature strokes overlapping printed characters using a Support Vector Machine (SVM) and conditional random fields. Another system for automatic signature segmentation that uses SVMs, scale invariant feature transforms, and spatial pyramid matching is presented in [2].

A method for signature extraction from bilingual documents using the contour and blobs-based method is described in [4]. A document image analysis system which uses two classifiers is presented in [5]. Their proposed system is able to extract typed and handwritten text from documents of different types in various languages. The first classifier separates text from non-text and the second one identifies typed and handwritten text.

Markov random fields are used in [6] to separate typed and handwritten text. The use of conditional random fields was proposed for signature segmentation in [1]. Their proposed method separates overlapping handwritten and typed text by segmenting and classifying strokes using SVMs. Many other methods have been designed for extraction and verification of signatures [1], [7], [8], [9], [10]. All above methods have various degrees of success when it comes to separating signatures overlapping other document elements.

Modern spectral imaging techniques have proven their importance in medical imaging by providing new tools to medical specialists for diagnosing diseases [11], [12], [13], [14]. HSI has also been applied in many other fields, like in agriculture for improving cultivation efficiency and analyzing soil properties [15], [16], [17], [18].

In hyperspectral document imaging, each pixel in a document has its own spectral signature. Several mathematical tools that are used in hyperspectral sensors can also be applied to hyperspectral document images for classification, improving the legibility of deteriorated text, and for detecting doctored documents [15]. HSI techniques for document analysis can provide significant information to forensic examiners about the authenticity of documents. A multivariate HSI-based study was conducted in [16] to assess the effectiveness of HSI and chemometric techniques for detecting forgery in suspicious documents.

One technique for discovering document forgery is checking whether a document contains different types of ink. In [17], an HSI-based method is presented for determining whether a region of a document contains pixels of several types of ink and for classifying pixels according to ink type. An overview of applications of hyperspectral imaging in the fields of pattern recognition and forensic document examination is presented in [18].

In [19] a system was designed based on the speeded robust feature keypoint detection technique [20] that is able to segment signatures in HSI document images when the signatures do not overlap typed text or any other parts of a document. In [21] another signature segmentation method for HSI document images was proposed that uses a combination of two hyperspectral unmixing techniques: minimum volume simplex analysis (MVSA) and minimum volume enclosing simplex (MVES).

III. SPECTRAL UNMIXING OF HSI DOCUMENT IMAGES

In this paper we analyze hyperspectral images of documents with overlapping text and images through the use of end-member extraction methods. Before explaining an algorithms we first explain the essential terminology used in HSI analysis.

- **Spectral Channel:** A hyperspectral camera captures an image using many different wavelengths called spectral channels or bands.
- **Spectral Signature:** A spectral signature specifies the variations of reflected electromagnetic radiation captured for each pixel of an HSI image as a function of the wavelengths (see Figure 1).
- **Spectral Endmember:** A pixel in an HSI image might contain spectral signatures of several overlapping objects or components. The spectral signature of each one of these components is called a spectral endmember or just endmember.
- **Abundance Estimation:** The proportion of endmembers in a hyperspectral pixel is calculated by abundance estimation algorithms that construct an abundance map.

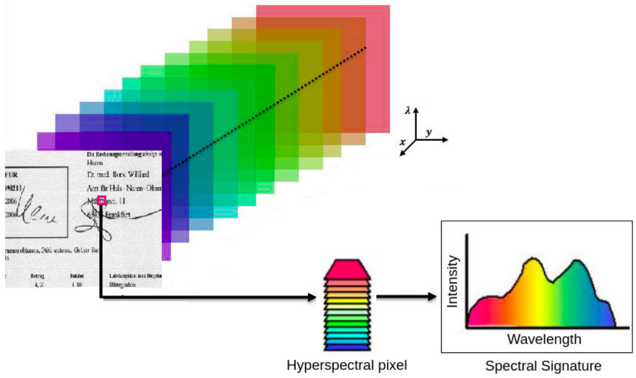

FIGURE 1. **A hyperspectral camera captures images consisting of a large number of channels. Each pixel has its own spectral signature.**

In spectral unmixing, an image is decomposed into its constituent spectral components (see Figure 2) and the spectral signature and abundance of their components is determined.

Hyperspectral images contain a great deal of data due to their large number of channels. To reduce the computational complexity of spectral unmixing algorithms, the data dimensions are first reduced. Spectral unmixing is generally divided into three steps: Dimension reduction, endmember extraction, and abundance estimation.

1) **Dimension Reduction:** As mentioned above, a hyperspectral image contains information for a large number of channels, however not all channels contain useful information; the channels that do not have useful information or are redundant channels. Before processing a hyperspectral image we detect and remove the redundant channels.
2) **Endmember Extraction:** The spectral information of each hyperspectral pixel is analyzed to determine the spectral endmembers.
3) **Abundance Estimation:** Once the spectral endmembers have been selected, the next step is to determine the fraction or relative weight of each endmember in the spectral signature of each pixel.

In this work we do not need to compute abundance estimation as part of the spectral unmixing process. Instead, we use end-member spectral information to extract handwritten signatures from documents as explained below.

A. METHODS FOR EXTRACTING ENDMEMBERS

Several algorithms for spectral endmember extraction have been developed, among them Pixel Purity Index (PPI) [22], Fast Interative PPI (FIPPI) [23], N-FINDR [24], and Automatic Target Generation Process (ATGP) [25].

- *Pixel Purity Index (PPI):* In this method the spectral signature of each pixel is represented as a vector of dimension equal to the number of spectral channels. A large number of random vectors called skewers is generated and the pixel vectors are projected onto each skewer. The pixels with largest projections are considered the endmembers. This method has several drawbacks including its random nature, sensitivity to the number of skewers, computational complexity, and the fact that manual verification of the selected set of endmembers is required.
- *Fast Iterative PPI (FIPPI):* This is an unsupervised algorithm that uses a combination of detection and classification techniques to build a suitable set of starting end-members. An iterative algorithm is then used to improve the set of end-members until some convergence criterion is satisfied. FIPPI is an improvement over PPI that overcomes some of its drawbacks.
- *N-FINDR:* This is another unsupervised algorithm that identifies endmembers based on the fact that the volume of the simplex formed by a vector representation of the endmembers has larger volume than the simplex defined by any other set of pixel vectors. The algorithm selects an initial simplex and repeatedly replaces pixel vectors in the simplex with vectors not in the simplex as long as the simplex volume increases.
- *Automatic Target Generation Process (ATGP):* ATGP is an unsupervised approach that projects each pixel vector onto a subspace orthogonal to the non-endmembers to select the most likely set of endmembers.

IV. SPECTRAL SIMILARITY METHODS

Spectral similarity methods compare the similarity between spectral signatures. The two most commonly used algorithms for spectral similarity are Spectral Angle Mapping (SAM) and Spectral Information Divergence (SID).

A. SPECTRAL ANGLE MAPPING

In Spectral Angle Mapping a pixel spectrum is represented as a vector with dimension equal to the number of spectral channels. A pixel vector has two components: its magnitude (length) and its angle. SAM compares two pixels by measuring the angle between its two corresponding pixel vectors so it is insensitive to errors caused by illumination effects [26].

B. SPECTRAL INFORMATION DIVERGENCE

Spectral Information Divergence (SID) considers a pixel as a random variable and defines a probability distribution for it according to its spectrum. The similarity between two pixels is computed as a relative entropy of their random variables [27].

V. HYPERSPECTRAL DOCUMENT METHODOLOGY

Our approach for extraction of signatures overlapping text or images in HSI images of documents is summarized in Figure 3. An HSI Document Image is first pre-processed using endmember extraction algorithms that yield vectors containing end-member spectral information. Later these vectors are used in HSI Image Regeneration methods like SAM & SID; the results are post processed to clean the

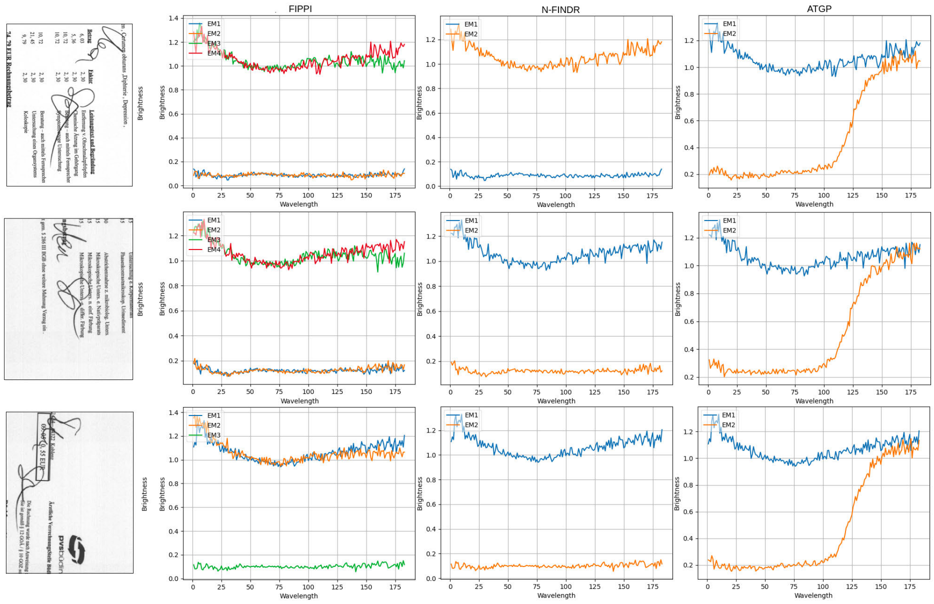

FIGURE 2. Spectral signatures generated by FIPPI, N-FINDR and ATGP, EM denotes endmember.

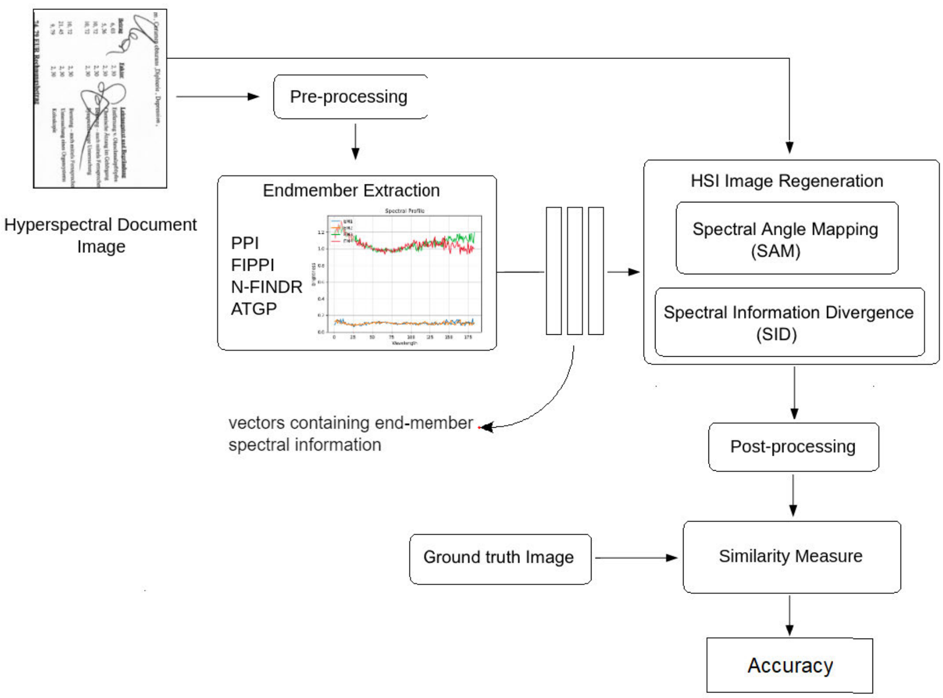

FIGURE 3. Methodology for the analysis of hyperspectral images of documents.

extracted signatures, and finally the accuracy of the extracted signatures is computed.

A. PRE-PROCESSING

The collection of HSI images that we used to test our algorithms consist of 59 HSI images, each one containing 240 channels and 800 x 640 pixels per channel. A visual inspection of the HSI images revealed that channels 0 to 15 and 200-240 do not contain information about the document signatures that had to be extracted and so we discarded these channels.

We added blur to the remaining 184 channels of each image as our experiments show that a slight blur on these channels allow us to obtain better results (see Figure 4).

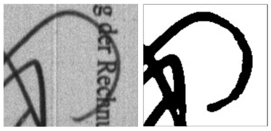

FIGURE 4. **Magnified view of a blurred image showing overlapped text and signature, and the recovered signature.**

Experiments performed without blurring recovered signatures that included many pixels that were not part of the signatures.

To apply blur we used the open-cv[1] library to convolve an image with a low-pass filter kernel. The filter kernel simply takes the average of all the pixels under the kernel area and replaces the central pixel with the average.

B. SPECTRAL UNMIXING

We used three methods for endmember extraction to compare their performance in overlapping text segmentation: FIPPI, N-FINDR, and ATGP. These methods produce endmembers that are grouped into classes (see Figure 2). Depending on the method, two, three, or four classes are produced. Endmember classes correspond to pixels belonging to typed text, pixels belonging to overlapped text and signature, pixels that belong to a signature, or pixels that belong to an image like a stamp or seal. The endmember classes are used to recover signatures as explained in the next section.

C. HSI SPECTRAL IMAGE REGENERATION

Spectral image regeneration means to recover a signature from a document by using the information produced by the end-member extraction algorithms. A signature is extracted by comparing each hyper-pixel of a document with the endmembers. Those pixels that have a high similarity with the endmembers belonging to signature and text-signature overlapping classes are considered as part of the signature and, hence, are part of the output. We used two different algorithms to compare pixels and endmembers: SAM and SID. A threshold similarity value is used with SAM and SID to select the pixels that are part of the output (see Figure 5). The value for this threshold needs to be adjusted manually by visually inspecting the recovered signatures.

D. POST-PROCESSING

The signature recovered using the above process might include noise that we remove in a post-processing step using a connected component-based method [28]. In a 2D image, connected components are clusters of pixels that have similar attributes and appear in adjacent positions. In post-processing, we examine the recovered signature and group its pixels into connected components based on pixel proximity and intensity similarity. Connected components with a number of pixels smaller than a pre-specified size are discarded from the final output (see Figure 6).

[1] https://pyimagesearch.com/2021/04/28/opencv-smoothing-and-blurring/

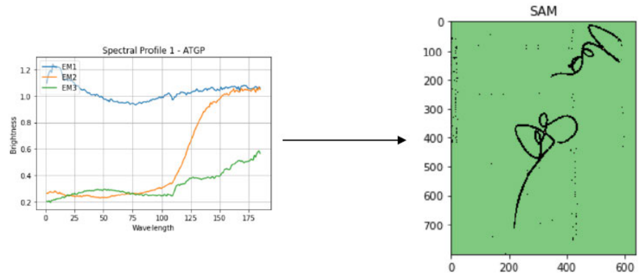

FIGURE 5. **Left: ATGP computes 3 groups of endmembers, Right: Signature extracted using ATGP and SAM before post-processing.**

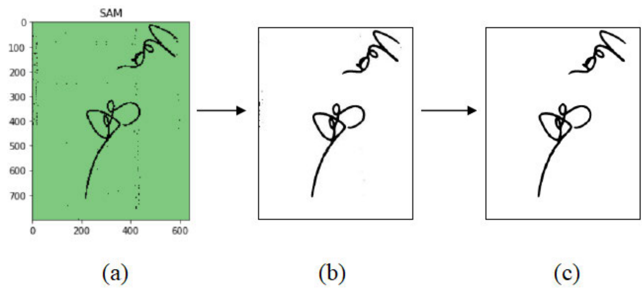

FIGURE 6. **(a) HSI image generated by SAM. (b) Image after post-processing (c) Ground truth.**

VI. EVALUATION METRICS

The signatures obtained after post processing were compared with the ground truth to determine the effectiveness of our algorithms. To compare the extracted signatures with the ground truth, we used the Structural Similarity Index Measure (SSIM).

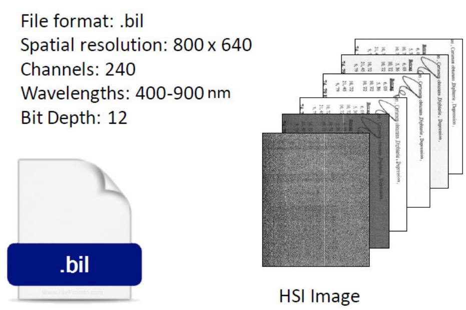

FIGURE 7. **HSI Image characteristics.**

A. STRUCTURAL SIMILARITY INDEX MEASURE

The Structural Similarity Index Measure is a metric which has been used by recent work on hyperspectral image analysis [3], [29]. SSIM provides a quantitative assessment of the similarity between two images. There are three parameters that are taken into account in order to calculate the SSIM of

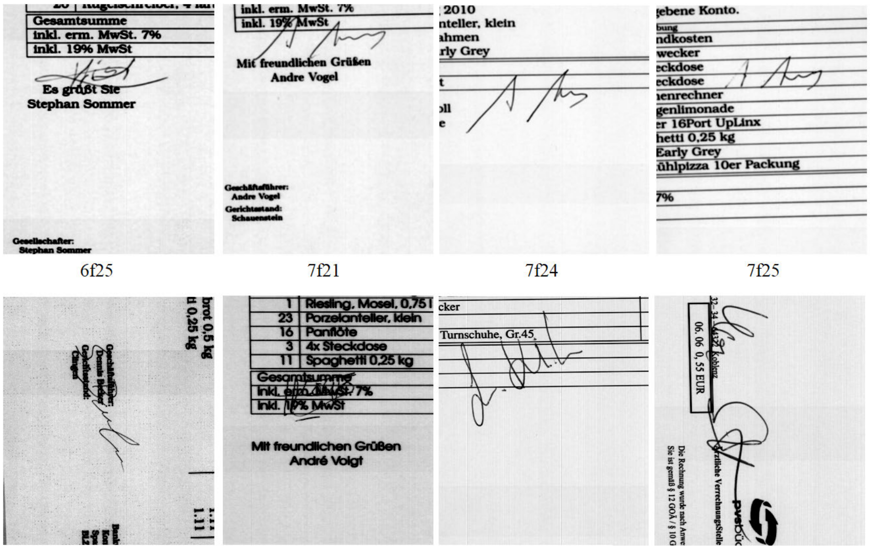

6f25 7f21 7f24 7f25

8f21 11f13 24Bf23 25Bg7

FIGURE 8. Sample of document regions showing signature overlapping typed text and/or images.

TABLE 1. Structural Similarity Index Measure (SSIM) for the set of images shown in Fig 8. Different endmember extraction algorithms (ATGP, FIPPI, and N-FINDR) and hyperspectral similarity algorithms (SAM and SID) were used. The maximum possible SSIM value is 1.

Blur filter size	Image	ATGP		FIPPI		NFINDR	
		SAM	SID	SAM	SID	SAM	SID
1 by 1	6f25	0.9262	0.9264	0.8601	0.8768	0.8728	0.8699
	7f21	0.9397	0.9407	0.9302	0.9338	0.9335	0.9443
	7f24	0.9371	0.9397	0.9366	0.9374	0.9207	0.9229
	7f25	0.8150	0.8092	0.7446	0.7594	0.7402	0.7590
	8f21	0.9577	0.9589	0.9405	0.9465	0.9392	0.9419
	11f13	0.7561	0.8240	0.7945	0.8175	0.8027	0.7945
	24Bf23	0.9558	0.9718	0.9058	0.9078	0.9099	0.9119
	25Bg7	0.9378	0.9410	0.9332	0.9344	0.9287	0.9341
2 by 2	6f25	0.9216	0.9347	0.9089	0.9313	0.9337	0.9321
	7f21	0.9351	0.9395	0.9302	0.9374	0.9314	0.9307
	7f24	0.9414	0.9467	0.9234	0.9239	0.9305	0.9398
	7f25	0.8138	0.8848	0.7770	0.8023	0.7714	0.7993
	8f21	0.9592	0.9607	0.9572	0.9594	0.9558	0.9567
	11f13	0.7787	0.8304	0.6571	0.7701	0.7461	0.7705
	24Bf23	0.9372	0.9522	0.9152	0.9435	0.9455	0.9643
	25Bg7	0.9367	0.9416	0.9312	0.9392	0.9273	0.9358
3 by 3	6f25	0.9354	0.9436	0.9265	0.9335	0.9279	0.9299
	7f21	0.9441	0.9554	0.8913	0.9509	0.9446	0.9554
	7f24	0.9613	0.9755	0.9389	0.9469	0.9382	0.9456
	7f25	0.8844	0.9228	0.8279	0.9039	0.7849	0.8047
	8f21	0.9599	0.9580	0.9407	0.9624	0.9521	0.9615
	11f13	0.8886	0.9143	0.8460	0.8619	0.8480	0.7615
	24Bf23	0.9833	0.9912	0.9722	0.9788	0.9799	0.9834
	25Bg7	0.9382	0.9476	0.9310	0.9422	0.9316	0.9425

two images: Luminance, contrast, and structural information. Luminance is the mean pixel intensity, and contrast is the standard deviation of pixel intensities. The structural information of an image is defined as those attributes of an image that are independent of the luminance and contrast. Hence, to compute the structural similarity of two images luminance is subtracted from pixel intensities and variance is normalized; then the correlation coefficient between the regularized pixels is defined as the structural similarity. The structural similarity index of two images is then a non-linear combination of luminance, contrast, and structural similarity. Using structural similarity index to compare two images has several advantages over error-sensitivity approaches (like the mean square error), including elimination of the following

FIGURE 9. Signature extracted using ATGP and SAM.

problems: Low correlation between image fidelity and image quality, the supra threshold problem, and the natural image complexity problem [30].

VII. EXPERIMENTAL ANALYSIS

A. HSI DOCUMENT IMAGE DATASET

As explained above, our dataset consists of 59 HSI document images captured by a UV-VIS hyperspectral[2] sensor. Each image has a spatial resolution of 800 × 640 pixels and each pixel is captured using 240 channels. Each of the 59 HSI images contains printed text and overlapping signatures. A few images also contain stamped seals overlapping the signatures. Each HSI image has the characteristics specified in Figure 7. HSI images are stored in files with the '.bil' extension, which is an abbreviation of 'band interleaved by line'; these are uncompressed files which contain the pixel values for each channel in the wavelength range of 400nm to 900nm. The number of bits per pixel per channel is 12.

B. EXPERIMENTAL SETUP

The endmember extraction algorithms described above are available in the pysptools[3] library. Each one of these algorithms receives as input an HSI image stored in a three dimensional array, and the number of endmember groups.

[2]https://www.headwallphotonics.com/products/uv-vis-250-500nm

[3]https://pysptools.sourceforge.io/eea.html

TABLE 2. SSIM for signature recovered from all 59 HSI images using ATGP and SID with different blur sizes.

Images	1 x 1	2 x 2	3 x 3
3d2	0.9453	0.938	0.9556
3d4	0.9504	0.9543	0.9597
4g1	0.917	0.934	0.9385
4g3	0.8698	0.9042	0.9012
4g4	0.8681	0.8875	0.89
4g8	0.8878	0.924	0.9317
5f22	0.9681	0.9319	0.8675
5g1	0.8875	0.9303	0.955
6f21	0.9106	0.8963	0.9121
6f22	0.9125	0.9165	0.9543
6f23	0.9239	0.9269	0.93
6f24	0.85	0.8498	0.8739
6f25	0.9264	0.9347	0.9436
7d5	0.9299	0.944	0.8824
7f21	0.9407	0.9395	0.9554
7f23	0.8992	0.9185	0.9464
7f24	0.9397	0.9467	0.9755
7f25	0.8092	0.8848	0.9228
7g1	0.9252	0.9382	0.9483
7g6	0.9406	0.9354	0.8475
7g7	0.9432	0.9468	0.866
7g8	0.9188	0.9308	0.9409
8f21	0.9589	0.9607	0.958
8f23	0.895	0.8758	0.9047
8f25	0.8916	0.9052	0.9144
11d8	0.9317	0.944	0.9816
11f11	0.7519	0.7785	0.7368
11f12	0.8406	0.8716	0.8903
11f13	0.824	0.8304	0.9143
11f15	0.7163	0.7008	0.6684
11f22	0.9274	0.9335	0.9449
11f25	0.965	0.9627	0.9757
11g2	0.8746	0.8743	0.8831
11g6	0.9629	0.957	0.9757
13g2	0.839	0.8598	0.8968
13g5	0.8312	0.8283	0.8217
23Bf22	0.9684	0.9612	0.9823
23Bf25	0.9591	0.9609	0.9865
24Bf21	0.9781	0.9741	0.9878
24Bf23	0.9718	0.9522	0.9912
24Bg6	0.9456	0.9523	0.9747
24Bg7	0.9662	0.9634	0.9688
25Bd6	0.9349	0.9539	0.9699
25Bd7	0.9153	0.9241	0.9723
25Bd8	0.929	0.9546	0.9748
25Bd9	0.9699	0.9711	0.973
25Bd10	0.9231	0.9471	0.9726
25Bf21	0.991	0.987	0.9914
25Bf22	0.9803	0.9558	0.9829
25Bf24	0.7904	0.8315	0.8443
25Bg2	0.9571	0.9614	0.9817
25Bg3	0.9445	0.9802	0.9845
25Bg4	0.9249	0.9345	0.9308
25Bg6	0.9727	0.978	0.9925
25Bg7	0.941	0.9416	0.9476
25Bg8	0.9669	0.9738	0.9898
25Bg9	0.9417	0.9481	0.9557

We have conducted experiments with different values for the number of endmember group for each endmember extraction algorithm. The best value for the number of endmembers was 3. ATGP and NFINDR produced the exact number of endmember groups as specified in the input, but FIPPI produced a different number of them due to the way in which FIPPI works.

SAM and SID receive as input the endmember spectral signatures, a 3D array storing an HSI image, and a threshold value between 0 and 1.

SAM determines the spectral similarity between two spectra by calculating the angle between their vector representations: Smaller angles represent higher similarity. SAM eliminates pixels that have value greater than the threshold value. In SID smaller divergence values correspond to higher similarity. Using SID, pixels with divergence value greater than the threshold are not part of the output.

We performed experiments with different threshold values for SAM and SID. Higher values for the threshold eliminated more signature pixels, so we determined that the best threshold value for SAM was 0.1. For SID we determined experimentally that the best value for the threshold was 0.009.

C. EXPERIMENTAL ANALYSIS

We performed experiments using different blur filter sizes and used both SAM and SID to recover the signatures. We selected blur filters of sizes 1×1, 2×2 and 3×3.

For our first set of experiments, we selected from our dataset a sample of 8 documents including some where the signature almost completely overlaps typed text and/or images and some where there is a small overlap of the signature with other parts of a document (see Figure 8). We used three endmember extraction algorithms on these documents: ATGP, FIPPI, and N-FINDR. Then we used both SAM and SID to recover the pixels of the signatures (see Figure 9.

For each recovered signature we computed the structural similarity index (SSIM) between the extracted signature and the ground truth. The experimental results are shown in Table 1. Note that the largest value for the SSIM is 1, indicating a perfectly recovered signature. The endmember extraction and hyperspectral similarity algorithms that produce the most consistent high quality results are ATGP and SID. Table 1 shows the performance of each endmember extraction technique and spectral similarity algorithms for different blur sizes.

In a second set of experiments, we used all the documents in our dataset. The results are shown in Table 2 using ATGP and SID and blur filter of different sizes. As mentioned earlier, experiments conducted without blurring produced lower quality results.

TABLE 3. Average SSIM for all 59 HSI documents for each endmember extraction algorithm, spectral similarity algorithm, and blur filter size.

Blur filter size	ATGP		FIPPI		NFINDR	
	SAM	SID	SAM	SID	SAM	SID
1 by 1	0.8988	0.9436	0.9149	0.8687	0.8816	0.9299
2 by 2	0.9082	0.9233	0.7681	0.9036	0.6652	0.7395
3 by 3	0.9174	0.9325	0.7680	0.9217	0.7076	0.8106

Table 3 shows the average SSIM for all 59 HSI documents for each end-member extraction algorithm (FIPPI, ATGP, NFINDR), spectral similarity index (SAM, SID), and blur filter size (1×1, 2×2 and 3×3).

VIII. CONCLUSION

Document analysis of hyperspectral images has a great potential in the field of forensic analysis. We propose a method for signature extraction in hyperspectral document images based on endmember extraction and hyperspectral similarity of hyper-pixels and endmembers. We implemented our method using three different endmember extraction algorithms and two hyperspectral similarity algorithms. Our experiments show that adding a slight blur to a hyperspectral document image helps segment signatures more accurately. We also proposed the use of Structural Similarity Index Measure to accurately compare extracted signatures with the ground truth, as this measure avoids some of the drawbacks of traditional error-sensitivity approaches. Our experimental results show that our method is able to recover with great precision signatures even from documents where the signature has significant overlap with other parts of the documents.

REFERENCES

[1] R. Mandal, P. P. Roy, and U. Pal, "Signature segmentation from machine printed documents using conditional random field," in *Proc. Int. Conf. Document Anal. Recognit.*, Sep. 2011, pp. 1170–1174.

[2] R. Mandal, P. P. Roy, U. Pal, and M. Blumenstein, "Signature segmentation and recognition from scanned documents," in *Proc. 13th Int. Conf. Intellient Syst. Design Appl.*, Dec. 2013, pp. 80–85.

[3] R. Zhu, F. Zhou, and J.-H. Xue, "MvSSIM: A quality assessment index for hyperspectral images," *Neurocomputing*, vol. 272, pp. 250–257, Jan. 2018.

[4] V. K. Gunjan and J. M. Zurada, Eds., *Modern Approaches in Machine Learning and Cognitive Science: A Walkthrough*. Cham, Switzerland: Springer, 2021.

[5] P. Barlas, S. Adam, C. Chatelain, and T. Paquet, "A typed and handwritten text block segmentation system for heterogeneous and complex documents," in *Proc. 11th IAPR Int. Workshop Document Anal. Syst.*, Apr. 2014, pp. 46–50.

[6] X. Peng, S. Setlur, V. Govindaraju, and R. Sitaram, "Handwritten text separation from annotated machine printed documents using Markov random fields," *Int. J. Document Anal. Recognit.*, vol. 16, no. 1, pp. 1–16, Mar. 2013.

[7] D. Impedovo and G. Pirlo, "Automatic signature verification: The state of the art," *IEEE Trans. Syst., Man, Cybern. C, Appl. Rev.*, vol. 38, no. 5, pp. 609–635, Sep. 2008.

[8] S. Ahmed, M. I. Malik, M. Liwicki, and A. Dengel, "Signature segmentation from document images," in *Proc. Int. Conf. Frontiers Handwriting Recognit.*, Sep. 2012, pp. 425–429.

[9] İ. Cüceloğlu and H. Oğul, "Detecting handwritten signatures in scanned documents," in *Proc. 19th Comput. Vis. Winter Workshop*, 2014, pp. 89–94.

[10] N. Sharma, R. Mandal, R. Sharma, U. Pal, and M. Blumenstein, "Signature and logo detection using deep CNN for document image retrieval," in *Proc. 16th Int. Conf. Frontiers Handwriting Recognit. (ICFHR)*, Aug. 2018, pp. 416–422.

[11] J. Yoon, "Hyperspectral imaging for clinical applications," *BioChip J.*, vol. 16, no. 1, pp. 1–12, Jan. 2022.

[12] S. Kumar, C. Desmedt, D. Larsimont, C. Sotiriou, and E. Goormaghtigh, "Change in the microenvironment of breast cancer studied by FTIR imaging," *Analyst*, vol. 138, no. 14, pp. 4058–4065, 2013.

[13] Z. Liu, H. Wang, and Q. Li, "Tongue tumor detection in medical hyperspectral images," *Sensors*, vol. 12, no. 1, pp. 162–174, Dec. 2011.

[14] K. Mitra, J. Melvin, S. Chang, K. Park, A. Yilmaz, S. Melvin, and R. X. Xu, "Indocyanine-green-loaded microballoons for biliary imaging in cholecystectomy," *J. Biomed. Opt.*, vol. 17, no. 11, Nov. 2012, Art. no. 116025.

[15] M. Liwicki, M. I. Malik, C. E. van den Heuvel, X. Chen, C. Berger, R. Stoel, M. Blumenstein, and B. Found, "Signature verification competition for online and offline skilled forgeries (SigComp2011)," in *Proc. Int. Conf. Document Anal. Recognit.*, Sep. 2011, pp. 1480–1484.

[16] C. S. Silva, M. F. Pimentel, R. S. Honorato, C. Pasquini, J. M. Prats-Montalbán, and A. Ferrer, "Near infrared hyperspectral imaging for forensic analysis of document forgery," *Analyst*, vol. 139, no. 20, pp. 5176–5184, 2014.

[17] Z. Luo, F. Shafait, and A. Mian, "Localized forgery detection in hyperspectral document images," in *Proc. 13th Int. Conf. Document Anal. Recognit. (ICDAR)*, Aug. 2015, pp. 496–500.

[18] Z. Khan, F. Shafait, and A. S. Mian, "Towards automated hyperspectral document image analysis," in *Proc. AFHA*, 2013, pp. 41–45.

[19] M. I. Malik, S. Ahmed, F. Shafait, A. S. Mian, C. Nansen, A. Dengel, and M. Liwicki, "Hyper-spectral analysis for automatic signature extraction," in *Proc. 17th Biennial Conf. Int. Graphonomics Soc. (IGS)*, 2015, pp. 1–4.

[20] H. Bay, A. Ess, T. Tuytelaars, and L. Van Gool, "Speeded-up robust features (SURF)," *Comput. Vis. Image Understand.*, vol. 110, no. 3, pp. 346–359, Jun. 2008.

[21] K. Iqbal and K. Khurshid, "Automatic signature extraction from document images using hyperspectral unmixing," in *Proc. Pakistan Acad. Sci., Pakistan Acad. Sci. A, Phys. Comput. Sci.*, vol. 54, no. 3, pp. 269–276, 2017.

[22] J. W. Boardman, F. A. Kruse, and R. O. Green, "Mapping target signatures via partial unmixing of AVIRIS data: In summaries," Tech. Rep., 1995.

[23] C.-I. Chang and A. Plaza, "A fast iterative algorithm for implementation of pixel purity index," *IEEE Geosci. Remote Sens. Lett.*, vol. 3, no. 1, pp. 63–67, Jan. 2006.

[24] X. Zhang, X.-H. Tong, and M.-L. Liu, "An improved N-FINDR algorithm for endmember extraction in hyperspectral imagery," in *Proc. Joint Urban Remote Sens. Event*, May 2009, pp. 1–5.

[25] H. Ren and C.-I. Chang, "Automatic spectral target recognition in hyperspectral imagery," *IEEE Trans. Aerosp. Electron. Syst.*, vol. 39, no. 4, pp. 1232–1249, Oct. 2003.

[26] J. A. Richards, *Remote Sensing Digital Image Analysis: An Introduction*. Berlin, Germany: Springer, 1986.

[27] C.-I. Chang, "Spectral information divergence for hyperspectral image analysis," in *Proc. IEEE Int. Geosci. Remote Sens. Symp. (IGARSS)*, vol. 1, Jun. 1999, pp. 509–511.

[28] A. Özlü. (2018). *Overlapped Handwritten Signature Extraction From Scanned Documents*. [Online]. Available: https://github.com/ahmetozlu/signature_extractor

[29] H. Ge, L. Wang, H. Pan, Y. Zhu, X. Zhao, and M. Liu, "Affinity propagation based on structural similarity index and local outlier factor for hyperspectral image clustering," *Remote Sens.*, vol. 14, no. 5, p. 1195, Feb. 2022.

[30] Z. Wang, A. C. Bovik, H. R. Sheikh, and E. P. Simoncelli, "Image quality assessment: From error visibility to structural similarity," *IEEE Trans. Image Process.*, vol. 13, no. 4, pp. 600–612, Apr. 2004.

HASAN IRTAZA MIRZA received the master's degree in computer science from the National University of Science and Technology, Islamabad, Pakistan, in 2022.

With his tenure as a Senior Full Stack Developer at SysReforms International Pvt Ltd., in January 2019, he has showcased his expertise in a range of languages and platforms. He is currently a Senior Full Stack Developer with SysReforms International, Islamabad. His skill set encompasses PHP, React JS, Python, Node.js, Java, C#, and Business Intelligence (BI), all of which he has successfully applied across diverse projects. In his capacity as a Team Lead, he led the development and testing of various high-end projects for UNFPA Pakistan and WHO EMRO Region, thereby demonstrating his leadership and technical skills. Previously, he held the position of the IT Expert/MIS Coordinator at the Population Program Wing, Ministry of National Health Services Regulations and Coordination, Islamabad, from May 2022 to December 2022. During this time frame, he made substantial contributions to the maintenance and enhancement of the "Web portal on reporting of CCI Action Plan" for UNFPA, utilizing React JS and PHP—Laravel. He also played an instrumental role in the development of the Population Program Wing Website, offering IT support, and analyzing data for various initiatives.

SAAD BIN AHMED received the master's degree in intelligent systems from Technische Universitaet, Kaiserslautern, Germany, in 2012, and the Ph.D. degree in computer sciences from Universiti Teknologi Malaysia, in 2019.

He has served as a Lecturer with King Saud bin Abdulaziz University for Health Sciences (KSAU-HS), Riyadh, Saudi Arabia, for seven years. He served as a Research Assistant with the Image Understanding and Pattern Recognition Research Group, Technische Universitaet. He is currently an Assistant Professor with Lakehead University, Thunder Bay, ON, Canada. He has accomplished his postdoctoral research from the University of Western Ontario, London, Canada. He is also the Director of the Image Analysis and Pattern Identification Research Laboratory (IAPI-RL). He is associated with various computer science journals and provides his expertise in reviewing novel contributions. By utilizing his extensive academic experience, he has significantly contributed which has been published as research articles in impact factor journals, conferences, and book chapters. His research interests include document image analysis, machine learning, computer vision, and optical character recognition. He is in the image analysis and pattern recognition field for 15 years and has been involved in various pioneer researches like collection of handwritten Urdu data and used it for Urdu character recognition. He provided his expertise in capturing Arabic scene text images and performing research on collected samples by machine learning and pattern recognition techniques. The focus of his research is on hyperspectral image analysis and explainable AI.

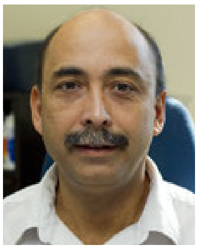

ROBERTO SOLIS-OBA received the Ph.D. degree from Purdue University, under the supervision of Prof. Greg Frederickson. He held a postdoctoral position at the Max Planck Institute for Informatics, under the guidance of Prof. Kurt Mehlhorn. The research of him centers on the design of efficient approximation algorithms for NP-hard optimization problems and he has conducted extensive research on network, scheduling, and packing optimization problems. He has been the Co-Founder of the Workshop on Approximation and Online Algorithms (WAOA) that has taken place annually, since 2003. He is currently a Professor with the Department of Computer Science, University of Western Ontario. He has served in the program committees of numerous conferences specialized on algorithm design. He received the Faculty Scholar Award and the USC Teaching Award from the University of Western Ontario.

MUHAMMAD IMRAN MALIK received the master's and Ph.D. degrees in machine learning from TU Kaiserslautern, Germany, in 2011 and 2015, respectively. He is currently the Head of the Computer Science Department, School of Electrical Engineering and Computer Science (SEECS), National University of Sciences and Technology (NUST). He has published around 70 peer-reviewed papers in leading international conferences and reputed journals. His research interests include forensic document analysis, signature and handwriting analysis, remote sensing, and hyper spectral imagery and analysis. He has jointly acquired funding of more than half a million Euros in different national and international research grants.